IEEE Access
Multidisciplinary | Rapid Review | Open Access Journal

Date of publication xxxx 00, 0000, date of current version xxxx 00, 0000.

Digital Object Identifier 10.1109/ACCESS.2017.DOI

Model-Free Predictive Current Control of a Voltage Source Inverter

JOSE RODRIGUEZ[1], (Fellow, IEEE), RASOOL HEYDARI[2], (MEMBER, IEEE), ZAHRA RAFIEE[3], HECTOR YOUNG[4], (MEMBER, IEEE), FREDDY FLORES-BAHAMONDE[1], (MEMBER, IEEE) AND MAHDI SHAHPARASTI[2], (Senior Member, IEEE)

[1]Department of Engineering Science, Universidad Andres Bello, Providencia - Santiago - Chile (e-mail: jose.rodriguez@unab.cl, freddy.flores@unab.cl)
[2]Electrical Engineering, Mads Clausen Institute, University of Southern Denmark, Odense, DK, 5230, Denmark, e-mail: (rah@sdu.dk, mshah@sdu.dk)
[3]Faculty of Electrical Engineering, Shahid Beheshti University, Tehran, Iran, e-mail: (z_rafiee@sbu.ac.ir)
[4]Department of Electrical Engineering, Universidad de La Frontera, Temuco 4811230, Chile

Corresponding author: Freddy Flores-Bahamonde (e-mail: freddy.flores@unab.cl).

J. Rodriguez acknowledges the support of ANID through projects FB0008, 1170167 and Anillo Project ACT192013. F. Flores-Bahamonde acknowledges the support of SERC Chile (CONICYT/FONDAP/15110019).

ABSTRACT Conventional model predictive control (MPC) of power converter has been widely applied to power inverters achieving high performance, fast dynamic response, and accurate transient control of power converter. However, the MPC strategy is highly reliant on the accuracy of the inverter model used for the controlled system. Consequently, a parameter or model mismatch between the plant and the controller leads to a sub-optimal performance of MPC. In this paper, a new strategy called model-free predictive control (MF-PC) is proposed to improve such problems. The presented approach is based on a recursive least squares algorithm to identify the parameters of an auto-regressive with exogenous input (ARX) model. The proposed method provides an accurate prediction of the controlled variables without requiring detailed knowledge of the physical system. This new approach and is realized by employing a novel state space identification algorithm into the predictive control structure. The performance of the proposed model-free predictive control method is compared with conventional MPC. The simulation and experimental results show that the proposed method is totally robust against parameters and model changes compared with the conventional model based solutions.

INDEX TERMS Model-free predictive control, MPC, robustness, voltage source converter

I. INTRODUCTION

THE high penetration of generators, loads and storage systems to the main grid, turns power converters and control architectures as main components for a more reliable operation. In addition to the energy transformation more challenging control objectives are demanded according to the needs of modern electrical systems. This is the case, for instance, of grid-connected systems such as renewable energy, electric drives in industrial applications, or electric transportation [1].

Conventionally, current and voltage control in inverters is based on linear controllers such as proportional-integral (PI), proportional-integrator-derivative (PID), and proportional resonant (PR) controllers, in addition to Pulse-Width Modulation (PWM) [2]–[5]. However, this linearized control structure has inherent low dynamic response [6].

In recent years, Finite-Control-Set Model Based Predictive Control (FCS-MPC) has gained increased attention controlling power converters for low, medium and high power applications [7], [8]. Advantages such as flexibility, high-speed response, straightforward constraint handling, multi-objective control capabilities and simple implementation have made MPC an interesting control approach for the community and even the industry [5], [6], [9]–[12]. As is well-known, to select the most appropriate control action for the converter a prediction of the future behavior of the system is realized based on a specific model that represent such system. However, due to its dependence on a mathematical model of the system, the performance of FCS-MPC is affected by parameter changes or model uncertainty, particularly in steady-state [11]. Different practical aspects limit the precision of the prediction model, such as unforeseen load changes, temperature variation or component aging. To improve the robustness of FCS-MPC when facing model uncertainties, different approaches have been proposed recently, creating

This article has been accepted for publication in a future issue of this journal, but has not been fully edited. Content may change prior to final publication. Citation information: DOI 10.1109/ACCESS.2020.3039050, IEEE Access

a new class of model-free predictive controllers.

Model-free predictive current control based on the analysis of current increments, assuming a linear behavior of the current between sampling intervals is presented in [13]–[16]. Model-free prediction methods based on past measurements of the effects of each inverter voltage vector, which are dynamically stored in a look-up table, have been proposed [17]. However, the update frequency of the measurements associated with each vector is critical to the performance and even the system stability.

In order to relax the dependency on unknown model parameters, the concept of ultra-local model has been applied, where predictions are made using a dynamic model that is continuously adapted based on the input-output behavior of the system [18], [19]. A drawback of this method is the need of tuning several parameters in the prediction model. An improvement was proposed in [20], using an ultra-local model structure with an extended state observer to predict the system behavior.

Online identification of inductance in the interior permanent magnet synchronous motor (IPMSM) using and adaptive observer with a recursive algorithm has been proposed [21]. Other parameters can be also identified, but this require some modifications. The identification algorithm is included in the predictive algorithm, therefore reducing the number of calculations. However, the method is designed for a specific application (IPMSM), so it can not be readily applied to systems with a different structure. Adaptation mechanisms based on recursive least squares (RLS) estimation have been recently proposed [22]. A limitation of this approach is that the structure of the system is established by the application, i.e., a synchronous motor. Therefore, adapting the method to a different system configuration is not straightforward.

In order to improve the performance of the predictive controller under uncertainty in the load model, an autoregressive with exogenous input (ARX) structure has been used as a disturbance estimator [23]. However, the ARX structure was used in combination with a conventional prediction model that still demands detailed knowledge of the physical structure of the controlled system.

From the review of existing model-free predictive control strategies we note the need for a systematic approach to construct the prediction model without previous knowledge of the physical system. This implies not only uncertainty in the parameter values, but also on the structure of a mathematical model. In this paper, a novel model-free predictive control (MF-PC) is proposed, where the RLS algorithm is employed to identify the parameters of a generic ARX model. The main contributions of this approach are:

1) A systematic procedure to design a model-free control strategy based on parameter identification of a generic mathematical model using the RLS algorithm.

2) The proposed approach does not require a detailed knowledge of the physical system, and inherently adapts the prediction model using measured data of the process. This makes the controller exceptionally robust to load changes or parameter mismatch.

3) By maintaining the direct control principle of FCS-MPC, the proposed MF-PC is able to retain the very fast dynamic response of this class of controller.

The rest of this paper is organized as follows. Section II presents a brief introduction to conventional FCS-MPC, and the effect of model parameter mismatch on the performance of the classical MPC approaches. Details of the proposed model-free predictive control algorithm are given in Section III. Simulation and experimental results of the proposed approach are demonstrated in Section IV. Finally, Section V concludes the paper.

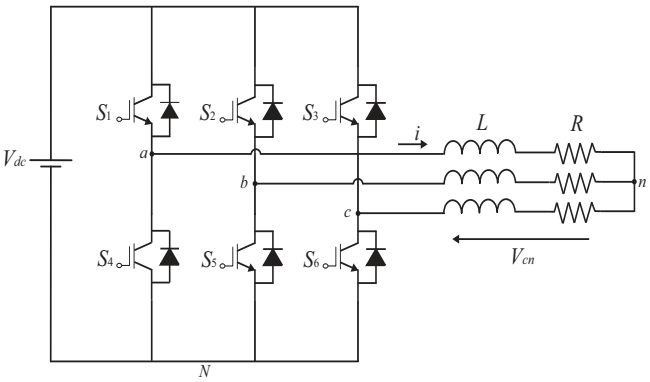

FIGURE 1: Generic model of a voltage source inverter.

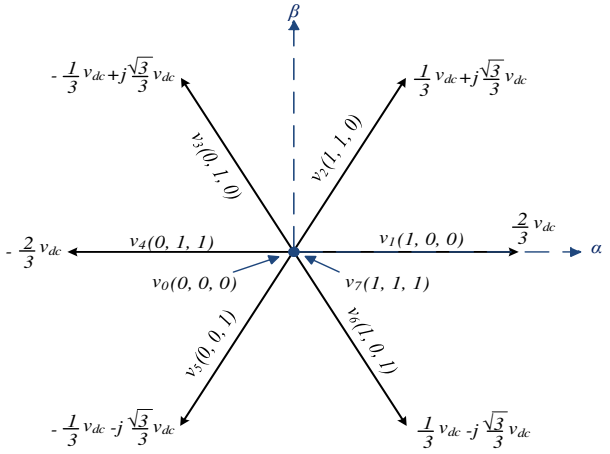

FIGURE 2: Voltage vectors and switching states generated by a two-level three-phase VSI.

II. CONVENTIONAL FCS-MPC

In general, FCS-MPC algorithms take advantage of the reduced number of switching states that can be generated in electronic power converters, which makes possible to use exhaustive search techniques to select the optimal state in terms of given control requirements.

This article has been accepted for publication in a future issue of this journal, but has not been fully edited. Content may change prior to final publication. Citation information: DOI 10.1109/ACCESS.2020.3039050, IEEE Access

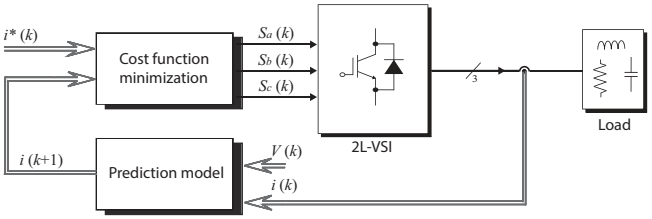

FIGURE 3: Classical Model Predictive Control Scheme.

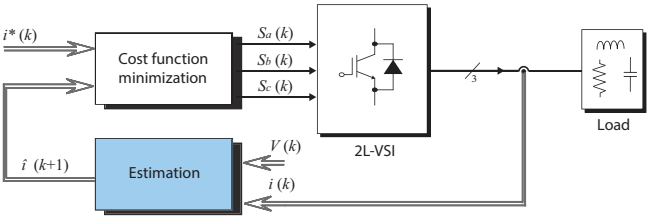

FIGURE 4: Proposed Model-Free Predictive Control Scheme.

The generic power circuit of a simple three-phase, two-level voltage-source inverter (2L-VSI) is shown in Fig. 1. The different eight voltage switching states of the converter are determined by the gating signals, i.e., S_a, S_b, and S_c as shown in Fig. 2, and expressed in vectorial form by

$$\mathbf{S} = \frac{2}{3}(S_a + \mathbf{a}S_b + \mathbf{a}^2 S_c) \tag{1}$$

where $\mathbf{a} = e^{j\pi/3}$. Each switching state defines a set of phase voltages of the inverter with respect to the negative bus-bar N, resulting in an output voltage state vector generated by the inverter defined by

$$\mathbf{v} = \frac{2}{3}(v_{aN} + \mathbf{a}v_{bN} + \mathbf{a}^2 v_{cN}) \tag{2}$$

Finally, the load current dynamics can be described by the vector equation

$$\mathbf{v} = R\mathbf{i} + L\frac{d\mathbf{i}}{dt}, \tag{3}$$

where R and L are the resistance and inductance of the three-phase load in Fig. 1, respectively, and $\mathbf{i}$ is the load current vector.

A discrete-time model of the load current (3) is employed to predict future values of the load current at the sampling instant $k+1$, for each one of the eight available voltage vectors $v(k)$ generated by the 2L-VSI, shown in Fig. 2. Without loss of generality, here we discuss the prediction model commonly employed for current control in RL loads, using Euler's method for discretization and represented in the complex $\alpha\beta$ frame [24]:

$$\begin{bmatrix} i_\alpha^p(k+1) \\ i_\beta^p(k+1) \end{bmatrix} = \left(1 - \frac{RT_s}{L}\right) \begin{bmatrix} i_\alpha(k) \\ i_\beta(k) \end{bmatrix} + \frac{T_s}{L} \begin{bmatrix} v_\alpha(k) \\ v_\beta(k) \end{bmatrix}, \tag{4}$$

where the superscript p denotes the predicted variables and T_s is the sampling period. For computing the predicted currents in (4), instantaneous measurement of load currents $i_\alpha(k)$, $i_\beta(k)$ and the components of the complex voltage vector applied to the load $v_\alpha(k)$ and $v_\beta(k)$ are required. The model parameters are the load resistance R and inductance L.

The control objectives for FCS-MPC algorithms are expressed in a cost function, which is a measure of the degree of accomplishment of each switching state of the inverter regarding the desired system behavior. In the case of current control, where the objective is to track of a current reference with components i_α^* and i_β^*, the cost function is defined as:

$$g_i = |i_\alpha^*(k+1) - i_\alpha^p(k+1)|^2 + |i_\beta^*(k+1) - i_\beta^p(k+1)|^2 \tag{5}$$

A block diagram of the conventional MPC strategy applied to a 2L-VSI inverter described in Fig. 1 is illustrated in Fig. 3. However, the main drawback of the conventional FCS-MPC approach is the dependence on the model quality in the prediction equation (4). Modeling errors can be generally ascribed to parametric and non-parametric uncertainty with respect to the real physical system. Parametric uncertainty arises from an incomplete knowledge of accurate values of parameters in the model, whereas non-parametric uncertainty is related to neglected dynamics, measurement noise or sensor dynamics [25].

The negative effect of model uncertainty on the performance of model predictive algorithms is well known. Particularly, in the case of FCS-MPC it has been demonstrated that prediction error has a complex relationship with parametric uncertainties, depending also on the instantaneous values of electrical parameters [26]. To overcome the aforementioned problem with conventional FCS-MPC, a model-free predictive control is proposed, and discussed in the following section.

III. PROPOSED MODEL-FREE PREDICTIVE CONTROL STRUCTURE

As discussed in section II, the objective of a predictive current control strategy is to minimize the error between a reference current and its measured values, which is implemented using a cost function such as (5). Note that in the conventional FCS-MPC, the current predictions are computed using a load or filter model, therefore, any uncertainty in the model leads to inaccurate current predictions, and consequently degrade the performance of the controller.

The motivation behind the proposed model-free predictive controller, illustrated in Fig. 4, is to reduce as much as possible the knowledge of the system required to perform predictions and compute optimal control actions. To achieve this, a mathematical model with a standard structure is selected, so that minimal previous knowledge of the physical system is needed. Then, by using an estimation algorithm, the parameters of the model are automatically updated using input and output measurements.

This article has been accepted for publication in a future issue of this journal, but has not been fully edited. Content may change prior to final publication. Citation information: DOI 10.1109/ACCESS.2020.3039050, IEEE Access

The main difference of the proposed controller with respect to the conventional FCS-MPC is the approach employed to obtain current predictions. The prediction model in Fig. 3 is built assuming that a detailed knowledge of the physical system is available, and its performance is affected if this premise is not fulfilled. On the other hand, the proposed controller represented in Fig. 4 uses an estimation algorithm to keep track of unmodeled dynamics or parameter changes in the physical system. The cost function for the proposed approach follows the same structure than the conventional FCS-MPC:

$$g_{\text{MF}} = |i^*_\alpha(k+1) - \hat{i_\alpha}(k+1)| + |i^*_\beta(k+1) - \hat{i_\beta}(k+1)|, \tag{6}$$

where, $i^*_\alpha(k+1)$ and $i^*_\beta(k+1)$ are the real and imaginary parts of the reference current, extrapolated to the future sampling period $k+1$. On the other hand, $\hat{i_\alpha}(k+1)$ and $\hat{i_\beta}(k+1)$ are the real and imaginary parts of the load current vector, predicted for the next sampling period using the estimated load model for a given inverter voltage vector.

Note that more complex cost functions considering system constraints are also presented in the literature [6], [27]. However, the basic cost function for current reference tracking is applied here for comparing the performances of the proposed method and the conventional FCS-MPC.

A. SYSTEM REPRESENTATION USING AN AUTOREGRESSIVE STRUCTURE

In a model-free approach, the filter and load system shown in Fig. 1 is treated as a black box, where the system model structure and parameters first have to be determined, so that predictions can be made. Among the several existing structures aimed to represent a dynamic system using linear models, the ARX stands out as one of the most widely employed. The extended use of ARX models is mainly explained because its parameters are simple to compute using well-established estimation algorithms such as RLS. Moreover, ARX models have a good performance even in the presence of small unmodeled non-linear effects, thus increasing the robustness of the prediction [28]. Therefore, in this work we use an ARX structure as the basis of the black-box model for the proposed predictive controller.

A transfer function between the output and input of the unknown system, represented using the ARX structure in the $\alpha-\beta$ stationary reference frame, is defined as follows:

$$\hat{i_\alpha}(k) = \frac{B^{\alpha\alpha}(z^{-1})}{A^{\alpha}(z^{-1})} v_\alpha(k) + \frac{B^{\alpha\beta}(z^{-1})}{A^{\alpha}(z^{-1})} v_\beta(k) \tag{7}$$

$$\hat{i_\beta}(k) = \frac{B^{\beta\alpha}(z^{-1})}{A^{\beta}(z^{-1})} v_\alpha(k) + \frac{B^{\beta\beta}(z^{-1})}{A^{\beta}(z^{-1})} v_\beta(k), \tag{8}$$

where $\hat{i_\alpha}(k)$ and $\hat{i_\beta}(k)$ are the estimated values of the load current, whereas $v_\alpha(k)$ and $v_\beta(k)$ are the voltages generated by the VSI and constitute the inputs to the unknown system to be controlled. The polynomials in the ARX model are defined as:

$$A^i(z^{-1}) = 1 + a^i_1 z^{-1} + a^i_2 z^{-2} + \ldots + a^i_{n_A} z^{-n_A} \tag{9}$$

$$B^{ij}(z^{-1}) = b^{ij}_1 z^{-1} + b^{ij}_2 z^{-2} + \ldots + b^{ij}_{n_B} z^{-n_B}, \tag{10}$$

where superscript i of polynomials $B^{ij}(z^{-1})$ denote the axis (α or β) of the current being modeled, and j indicates the axis of the voltage acting as an external input. In the case of polynomials $A^i(z^{-1})$, superscript i indicates the axis of the estimated current. The order of the polynomials in the ARX structure is given by n_A and n_B. A and B are Matrix Polynomials proportional to z, which define the system model based on the correlation between the black box output and input vectors. Therefore, if the transfer function between input and output (7) and (8) can be identified accurately, the system model will be generated with no need to know about the complete model of the system.

A design aspect that influences both the ability of the ARX model to faithfully represent the system dynamics, and the computational burden of the control algorithm is the polynomial orders n_A and n_B in (9) and (10), respectively. There is a trade-off where higher polynomial order increases the model flexibility for capturing complex phenomena, but on the other hand unnecessarily high orders can increase the computational burden and complexity of algorithms based on the ARX model [29]. Considering the system illustrated in Fig. 1, in this paper we selected $n_A = 3$ and $n_B = 2$ in order to achieve a good control performance and low computational burden.

B. RLS PARAMETER ESTIMATION ALGORITHM

The RLS algorithm has a long history in parameter estimation for control applications [30]. It is mainly employed to obtain a reliable dynamic model of systems subject to structure or parameter uncertainty, or time-varying characteristics. Hence, in this paper we propose to use the RLS algorithm to compute the coefficients of the ARX model given by (7) and (8) using measurements obtained from the controlled system.

The RLS algorithm consists of a set of equations that is solved recursively, where the objective at each iteration is to obtain an accurate estimation of the parameters vector at the present time $\hat{\boldsymbol{\theta}}(k)$:

$$\begin{aligned} \hat{\boldsymbol{\theta}}(k) &= \hat{\boldsymbol{\theta}}(k-1) + \boldsymbol{G}(k)e(k) \\ \boldsymbol{G}(k) &= \frac{\boldsymbol{P}(k-1)\boldsymbol{\varphi}(k)}{\boldsymbol{\varphi}^T(k)\boldsymbol{P}(k-1)\boldsymbol{\varphi}(k) + \lambda} \\ \boldsymbol{P}(k) &= \frac{1}{\lambda}\left(\boldsymbol{I} - \boldsymbol{G}(k)\boldsymbol{\varphi}^T(k)\right)\boldsymbol{P}(k-1). \end{aligned} \tag{11}$$

The gain matrix $\boldsymbol{G}(k)$ links the updated parameters vector at each sampling step with estimation error $e(k)$ given by:

$$e(k) = i(k) - \boldsymbol{\varphi}^T(k)\hat{\boldsymbol{\theta}}(k-1), \tag{12}$$

where $i(k)$ is the instantaneous current measurement. The forgetting factor $0 < \lambda \leq 1$ is introduced to give a higher

This article has been accepted for publication in a future issue of this journal, but has not been fully edited. Content may change prior to final publication. Citation information: DOI 10.1109/ACCESS.2020.3039050, IEEE Access

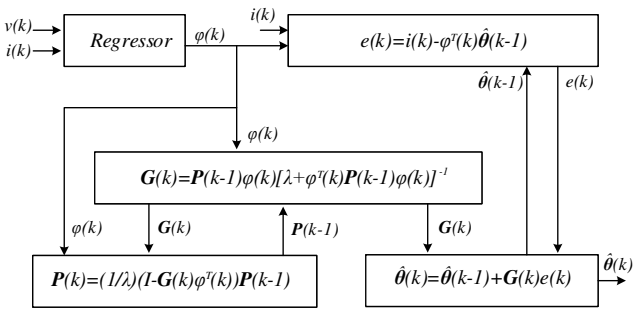

FIGURE 5: Block diagram of the RLS algorithm.

weighting to new measurements in the RLS algorithm [30]. Smaller values of λ lead to higher tracking velocity of fast-changing parameters, but make the system more sensitive to noise [31]. Since the sampling frequency in the implementation of the predictive controller is much higher compared to possible parametric variations, and to increase the noise immunity in this work we use $\lambda = 1$.

Vectors $\hat{\boldsymbol{\theta}}$ and $\boldsymbol{\varphi}$ in (11) and (12) are related to the controlled system as follows. First, estimated current equations (7) and (8) are rewritten as:

$$\begin{aligned}\hat{i}_\alpha(k) = &-a_1^\alpha i_\alpha(k-1) + \cdots - a_{n_A}^\alpha i_\alpha(k-n_A) + \\ &b_1^{\alpha\alpha} v_\alpha(k-1) + \cdots + b_{n_B}^{\alpha\alpha} v_\alpha(k-n_B) + \\ &b_1^{\alpha\beta} v_\beta(k-1) + \cdots + b_{n_B}^{\alpha\beta} v_\beta(k-n_B)\end{aligned} \tag{13}$$

$$\begin{aligned}\hat{i}_\beta(k) = &-a_1^\beta i_\beta(k-1) + \cdots + a_{n_A}^\beta i_\beta(k-n_A) + \\ &b_1^{\beta\alpha} v_\alpha(k-1) + \cdots + b_{n_B}^{\beta\alpha} v_\alpha(k-n_B) + \\ &b_1^{\beta\beta} v_\beta(k-1) + \cdots + b_{n_B}^{\beta\beta} v_\beta(k-n_B).\end{aligned} \tag{14}$$

Then, the unknown parameters to be identified in (13) and (14) are gathered in vectors $\boldsymbol{\theta}_1$ and $\boldsymbol{\theta}_2$, respectively:

$$\boldsymbol{\theta}_1 = [a_1^\alpha \dots a_{n_A}^\alpha b_1^{\alpha\alpha} \dots b_{n_B}^{\alpha\alpha} b_1^{\alpha\beta} \dots b_{n_B}^{\alpha\beta}]^T \tag{15}$$

$$\boldsymbol{\theta}_2 = [a_1^\beta \dots a_{n_A}^\beta b_1^{\beta\alpha} \dots b_{n_B}^{\beta\alpha} b_1^{\beta\beta} \dots b_{n_B}^{\beta\beta}]^T. \tag{16}$$

Similarly, the past data of input and output measurements in (13) and (14) is gathered in vectors $\boldsymbol{\varphi}_1$ and $\boldsymbol{\varphi}_2$, which are known as regressor vectors or explanatory variables and are given by:

$$\begin{aligned}\boldsymbol{\varphi}_1 = &[i_\alpha(k-1), \cdots, i_\alpha(k-n_A), \\ &v_\alpha(k-1), \cdots, v_\alpha(k-n_B), \\ &v_\beta(k-1), \cdots, v_\beta(k-n_B)]\end{aligned} \tag{17}$$

$$\begin{aligned}\boldsymbol{\varphi}_2 = &[i_\beta(k-1), \cdots, i_\beta(k-n_A), \\ &v_\alpha(k-1), \cdots, v_\alpha(k-n_B), \\ &v_\beta(k-1), \cdots, v_\beta(k-n_B)].\end{aligned} \tag{18}$$

Please note that the subscripts of vectors $\boldsymbol{\varphi}$ and $\hat{\boldsymbol{\theta}}$ have been omitted in (11) and (12). The RLS algorithm is computed independently using $\boldsymbol{\varphi}_1$ and $\boldsymbol{\varphi}_2$ to obtain the estimated parameters vectors $\hat{\boldsymbol{\theta}}_1$ and $\hat{\boldsymbol{\theta}}_2$, which are used to model the α and β axis of the load current, respectively.

A block diagram of the RLS algorithm is presented in Fig. 5. The inputs to the estimation algorithm, the instantaneous measured voltage and current applied to the load, are located in the top-left part of the diagram. The algorithm yields the estimated set of model parameters $\hat{\boldsymbol{\theta}}(k)$, as depicted in the bottom-right part of the figure. Therefore, the parameters of the transfer functions that define the system model are updated accurately at each sampling period.

C. STATE-SPACE REPRESENTATION AND PREDICTION

For the sake of convenience in the implementation of the proposed controller, the ARX system model in (7) and (8) is expressed as a state-space model in the observable canonical form:

$$\begin{aligned}x_\alpha(k+1) &= \underbrace{\begin{bmatrix} -a_1^\alpha & 1 & 0 & \cdots & 0 \\ -a_2^\alpha & 0 & 1 & \cdots & 0 \\ \vdots & \vdots & \vdots & \ddots & \vdots \\ -a_{n_A}^\alpha & 0 & 0 & \cdots & 0 \end{bmatrix}}_{A_\alpha} x_\alpha(k) + \\ &\quad + \underbrace{\begin{bmatrix} b_1^{\alpha\alpha} & b_1^{\alpha\beta} \\ \vdots & \vdots \\ b_{n_B}^{\alpha\alpha} & b_{n_B}^{\alpha\beta} \\ 0 & 0 \end{bmatrix}}_{B_\alpha} \begin{bmatrix} v_\alpha \\ v_\beta \end{bmatrix} \\ \hat{i}_\alpha(k) &= \underbrace{\begin{bmatrix} 1 & 0 & \cdots & 0 \end{bmatrix}}_{C_\alpha} x_\alpha(k)\end{aligned} \tag{19}$$

$$\begin{aligned}x_\beta(k+1) &= \underbrace{\begin{bmatrix} -a_1^\beta & 1 & 0 & \cdots & 0 \\ -a_2^\beta & 0 & 1 & \cdots & 0 \\ \vdots & \vdots & \vdots & \ddots & \vdots \\ -a_{n_A}^\beta & 0 & 0 & \cdots & 0 \end{bmatrix}}_{A_\beta} x_\beta(k) + \\ &\quad + \underbrace{\begin{bmatrix} b_1^{\beta\alpha} & b_1^{\beta\beta} \\ \vdots & \vdots \\ b_{n_B}^{\beta\alpha} & b_{n_B}^{\beta\beta} \\ 0 & 0 \end{bmatrix}}_{B_\beta} \begin{bmatrix} v_\alpha \\ v_\beta \end{bmatrix} \\ \hat{i}_\beta(k) &= \underbrace{\begin{bmatrix} 1 & 0 & \cdots & 0 \end{bmatrix}}_{C_\beta} x_\beta(k)\end{aligned} \tag{20}$$

The identified state-space model of the system, can be written as follows:

$$\begin{cases} x(k+1) = A_\alpha(k)x(k) + B_\alpha(k)\mathbf{v}(k) \\ \hat{i}_\alpha(k+1) = C_\alpha(k)x(k+1) \end{cases} \tag{21}$$

This article has been accepted for publication in a future issue of this journal, but has not been fully edited. Content may change prior to final publication. Citation information: DOI 10.1109/ACCESS.2020.3039050, IEEE Access

$$\begin{cases} x(k+1) = A_\beta(k)x(k) + B_\beta(k)\mathbf{v}(k) \\ \hat{i}_\beta(k+1) = C_\beta(k)x(k+1) \end{cases} \tag{22}$$

where, $\mathbf{v}(k) = [v_\alpha(k) \;\; v_\beta(k)]$ is the input voltage vector. Vectors C_α and C_β relate the predicted currents to the internal state $x(k+1)$, whereas matrices A_α, B_α, A_β and B_β contain the system model parameters and are updated using the RLS identification algorithm at each sampling time. Therefore, based on (21) and (22), a one-step ahead prediction of the output current is achieved.

Finally, the proposed predictive control algorithm is implemented as depicted in the flow chart of Fig. 6. During each sampling interval, the algorithm starts by applying the optimal inverter voltage vector computed in the preceding time step. Next, by using the instantaneous and past voltage and current measurements, the prediction model is estimated using the RLS method. The estimated model is updated continuously in order to keep track of any changes in the physical system, and is then used to predict the current at the future sampling period $k+1$ using (21) and (22). The cost function (6) is subsequently evaluated for each available inverter voltage and an exhaustive optimization method is used for selecting the optimal control action to be applied during the next sampling interval.

IV. SIMULATION AND EXPERIMENTAL RESULTS

In order to validate the performance of the proposed model-free predictive control structure, a simulated model in MATLAB/SimPowerSystems is compared with the conventional FCS-MPC proposed in [7]. The results are presented to highlight the effects of parameter mismatches, as well as model mismatch, between the modeled values of the load on the performance of the proposed MF-PC strategy compared to the conventional FCS-MPC. Furthermore, experimental result is provided to practically validate the performance of the proposed approach compared to the conventional FCS-MPC.

Fig. 7 shows the test system setup including oscilloscope, host PC and control desk, the power inverter connected to a three-phase load and OPAL-RT OP5700, which serves as an interface between the controller and the hardware. The test system parameters are presented in Table I. In order to implement the proposed MF-PC, the number of estimated parameters in the polynomials $A(z)$ and $B(z)$ are n_A=3, and n_B=2, respectively. Thus, based on (7) and (8) , the initial transfer function is determined as follows:

$$\begin{aligned} \hat{i}_\alpha(k) &= \frac{-6.51\times10^{-5}q^{-1}+5.29\times10^{-5}q^{-2}}{1-1.4163q^{-1}+0.0056q^{-2}+0.4106q^{-3}}v_\alpha(k) \\ &+ \frac{-1.87\times10^{-6}q^{-1}-4.87\times10^{-7}q^{-2}}{1-1.4163q^{-1}+0.0056q^{-2}+0.4106q^{-3}}v_\beta(k) \end{aligned} \tag{23}$$

$$\begin{aligned} \hat{i}_\beta(k) &= \frac{+1.89\times10^{-6}q^{-1}+9.73\times10^{-9}q^{-2}}{1-1.4651q^{-1}+0.0716q^{-2}+0.3935q^{-3}}v_\alpha(k) \\ &+ \frac{-6.32\times10^{-5}q^{-1}+5.51\times10^{-5}q^{-2}}{1-1.4651q^{-1}+0.0716q^{-2}+0.3935q^{-3}}v_\beta(k) \end{aligned} \tag{24}$$

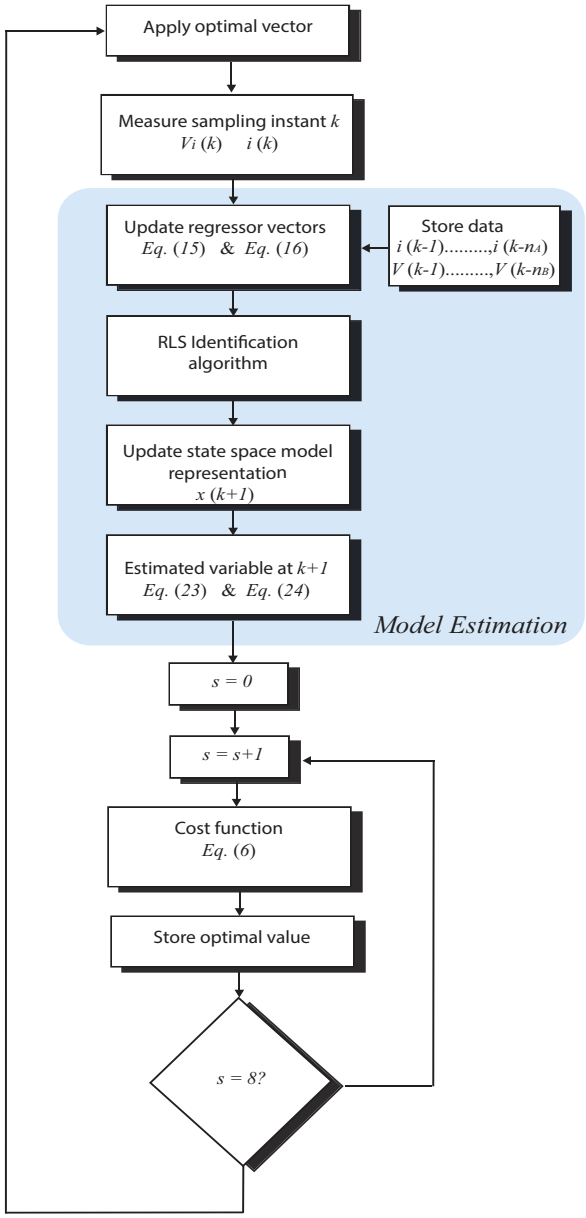

FIGURE 6: Proposed model-free control flow-chart.

Therefore, based on (21) and (22), the initial state-space model is obtained as follows:

$$\begin{aligned} x_\alpha(k+1) &= \underbrace{\begin{bmatrix} 1.4163 & 1 & 0 \\ -0.0056 & 0 & 1 \\ -0.4106 & 0 & 0 \end{bmatrix}}_{A} x_\alpha(k) + \\ &\underbrace{\begin{bmatrix} -6.51\times10^{-5} & -1.87\times10^{-6} \\ 5.29\times10^{-5} & -4.87\times10^{-7} \\ 0 & 0 \end{bmatrix}}_{B} \begin{bmatrix} v_\alpha \\ v_\beta \end{bmatrix} \\ \hat{i}_\alpha(k+1) &= \underbrace{[1 \;\; 0 \;\; 0]}_{C} x_\alpha(k) \end{aligned} \tag{25}$$

This article has been accepted for publication in a future issue of this journal, but has not been fully edited. Content may change prior to final publication. Citation information: DOI 10.1109/ACCESS.2020.3039050, IEEE Access

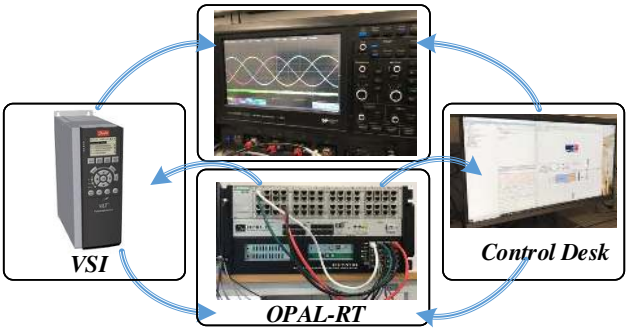

FIGURE 7: Experimental setup with voltage source inverter (VSI), oscilloscope, and OPAL-RT 5700 and control desk system for control.

$$
\begin{aligned}
x_\beta(k+1) &= \underbrace{\begin{bmatrix} 1.4651 & 1 & 0 \\ -0.0716 & 0 & 1 \\ -0.3934 & 0 & 0 \end{bmatrix}}_{A} x_\beta(k) + \\
&\underbrace{\begin{bmatrix} 1.89 \times 10^{-6} & -6.32 \times 10^{-5} \\ 9.73 \times 10^{-9} & 5.50 \times 10^{-5} \\ 0 & 0 \end{bmatrix}}_{B} \begin{bmatrix} v_\alpha \\ v_\beta \end{bmatrix} \\
\hat{i}_\beta(k+1) &= \underbrace{[1 \;\; 0 \;\; 0]}_{C} x_\beta(k)
\end{aligned}
\tag{26}
$$

It worth noting that the system model defined by the polynomials $A(z)$ and $B(z)$ are adaptively updated at each sampling time based on the system identification algorithm.

A. SCENARIO 1: TRANSIENT PERFORMANCE OF THE PROPOSED MF-PC

Fig. 8 shows the transient response of the proposed method. As can be seen, by changing the reference current at $t = 45\,\text{ms}$, the proposed MF-PC strategy follows the reference trajectory accurately, and very fast in several miliseconds. This fast transient response is the main achievement of the predictive control strategies. It is worth to note that the transient response of the conventional linear controller is much slower [6], [32]. Fig. 8a and Fig. 8b show the transient performance of the proposed approach for simulation and experimental results, respectively. As can be seen by employing the proposed MF-PC, the output current of VSI follows the reference trajectory very fast and accurate, without requiring previous knowledge of the system model or parameters. Thus, the proposed control strategy performance during transient time is also validated practically.

B. SCENARIO 2: PARAMETERS MISMATCH

In order to compare the results with the conventional FCS-MPC, parameters mismatch is carried out for both the conventional FCS-MPC and the proposed MF-PC. Fig. 9 shows the performance of the conventional FCS-MPC and MF-PC

TABLE 1: Test system parameters.

Parameter	Symbol	Value
DC Voltage	V_{dc}	520 V
Nominal voltage amplitude	V_{nom}	200 V
Nominal frequency	f_{nom}	50 Hz
Sampling time	T_s	10 μs
Nominal load current	i_{nom}	10 A
Nominal load resistance	R_0	10 Ω
Nominal load inductance	L_0	10 mH

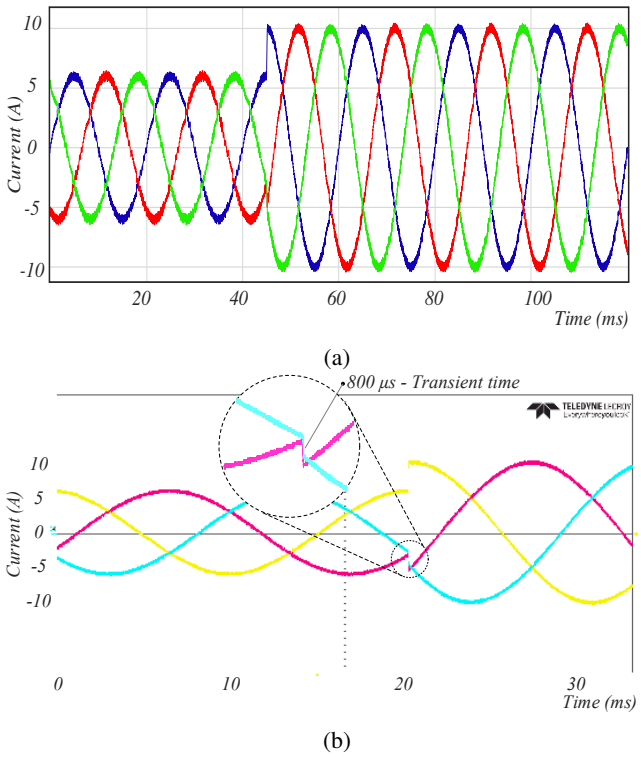

FIGURE 8: Results of the proposed MF-PC performance under current transient. (a) Simulation result. (b) Experimental result.

with accurate load parameters in the model. As can be seen, the output current for both control strategies is controlled accurately. However, the error between the reference current and the VSI output current in the MF-PC is lower. The main reason for this difference is that with the same sampling time, the proposed MF-PC shows a higher average switching frequency. To provide a fair baseline for the comparison between both predictive controllers, the sampling time of the conventional FCS-MPC is modified so that the average switching frequencies of both methods are the same. This case is shown in Fig. 10, where the error between the reference current and the VSI output current is very similar for both methods as the parameters of the prediction model for FCS-MPC are exactly known.

In the next step, a mismatch in parameters of the controller

This article has been accepted for publication in a future issue of this journal, but has not been fully edited. Content may change prior to final publication. Citation information: DOI 10.1109/ACCESS.2020.3039050, IEEE Access

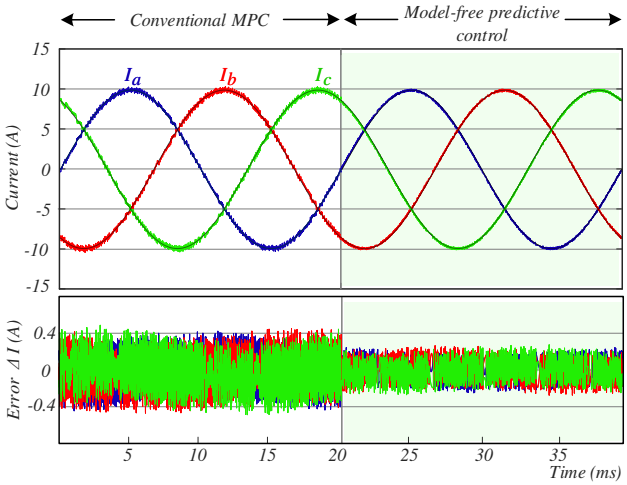

FIGURE 9: Compared simulation of the conventional FCS-MPC and the proposed MF-PC of voltage source inverter considering ideal model, with the same sampling time.

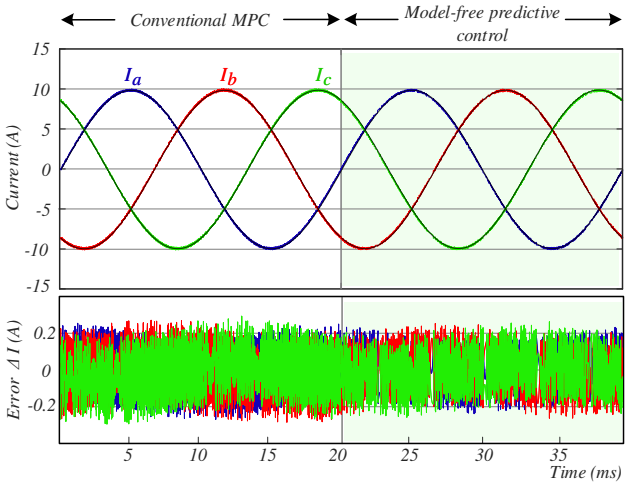

FIGURE 10: Compared simulation of the conventional FCS-MPC and the proposed MF-PC of voltage source inverter considering ideal model, with the same average switching frequency.

and the real value of the load is applied. In this case, the load inductance is two times larger than the model parameters, and the load resistance is two times smaller than the model parameters. In this scenario, the model is considered to be the same as the connected RL load with mismatch in the model parameters. As can be seen from Fig. 11, the parameters mismatches in the conventional FCS-MPC degrade the performance of the controller. The main reason is that the conventional FCS-MPC relies on the model of the system, and if the model is not accurate, the controller cannot perform well. However, as can be seen from Fig. 11 after $t = 20\,\mathrm{ms}$, when the MF-PC is activated, the error between the reference current and output current of VSI is lower than the conventional FCS-MPC, and the performance of the controller is much superior compared to the FCS-MPC.

These results are also validated experimentally. Fig. 8b and Fig. 11b shows the performance of the conventional model predictive control of VSI and the proposed approach, respectively. As can be seen from Fig. 8b and Fig. 11b, the proposed MF-PC has lower error, and much superior performance compared to the conventional FCS-MPC with parameters mismatch.

C. SCENARIO 3: MODEL MISMATCH

In this scenario an RLC load is applied to serve as the model mismatch. The predefined model of FCS-MPC is based on the RL load, and by employing an RLC load, the model of the system is totally different. Fig. 12 shows a comparison between the conventional FCS-MPC and the proposed MF-PC. As can be seen, by changing the model of the system, the conventional FCS-MPC is unstable. However, the proposed controller is independent to the system model, and changing the model has no effect on the performance of the controller.

Experimental results also validate this achievement. Fig. 12b shows the performance of the conventional FCS-MPC considering model mismatch. As it can be seen, when a model mismatch is applied, the system goes to instability. The reason is that the conventional FCS-MPC needs to have the model of the system to accurately predict the output current of the VSI and consequently control the switching states of the inverter. However, the proposed approach is totally model-free, and it could adaptively define the model of the system. Thus, as can be seen from Fig. 12c, the system is stable even when the model is changed.

D. AVERAGE SWITCHING FREQUENCY

The average switching frequency for the conventional MPC is around 8200 Hz and for the proposed model free predictive control is around 9500 Hz, which is calculated as follows [6]:

$$f_{\text{average}} = \frac{\sum_{i=1}^{N} sw(i)}{3\,N\,T_s}. \tag{27}$$

where, N is the total number of samples, and T_s is the sampling time.

Even though the average switching frequency obtained with MF-PC is not unusually high, there exist well-known approaches to reduce the switching activity by means of an additional term in the cost function that penalizes the switching effort [6]. However, in this paper we focused on a simple cost function structure in order to highlight the proposed controller's capability to operate under strong modeling uncertainty and to compare its performance with the conventional approach.

E. COMPUTATION TIME OF THE CONTROL ALGORITHM.

An important aspect that determines the feasibility of a control algorithm is the associated computational burden. Besides the prediction and optimization stages, which are the basis of the MPC strategy, the proposed MF-PC algorithm

This article has been accepted for publication in a future issue of this journal, but has not been fully edited. Content may change prior to final publication. Citation information: DOI 10.1109/ACCESS.2020.3039050, IEEE Access

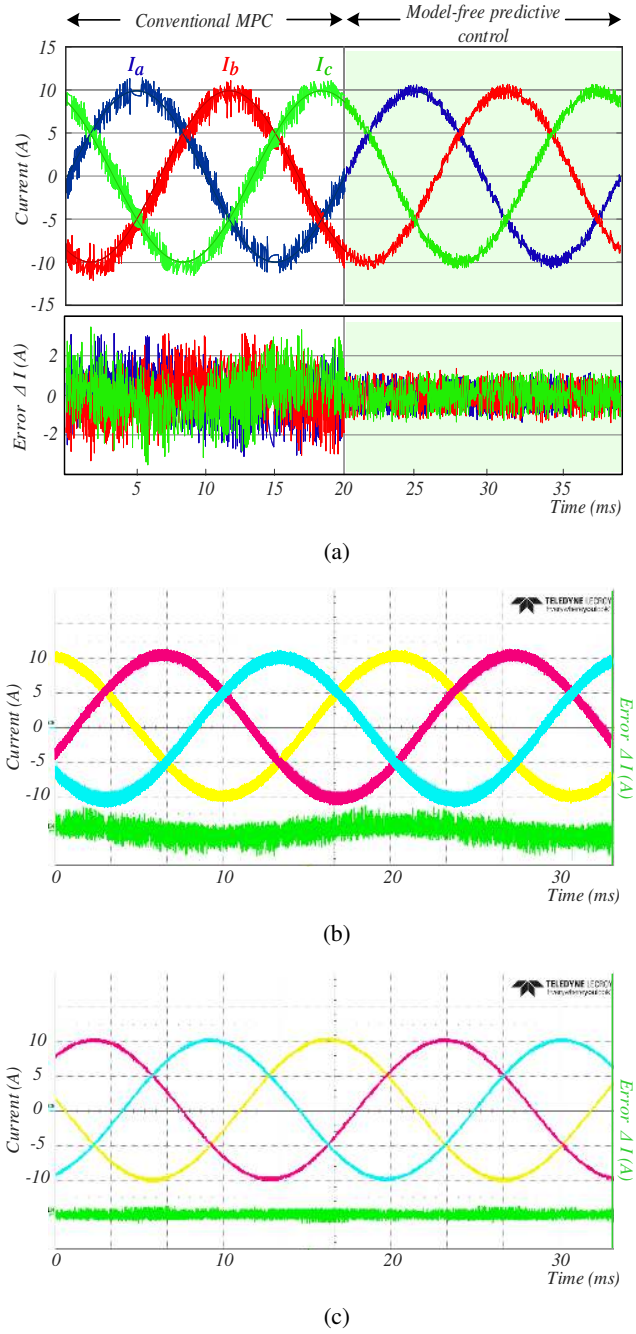

FIGURE 11: Comparison of conventional FCS-MPC and the proposed MF-PC of a voltage source inverter considering model parameter mismatch. (a) Compared simulation results of both controllers. (b) Experimental validation for conventional FCS-MPC. (c) Experimental validation for MF-PC.

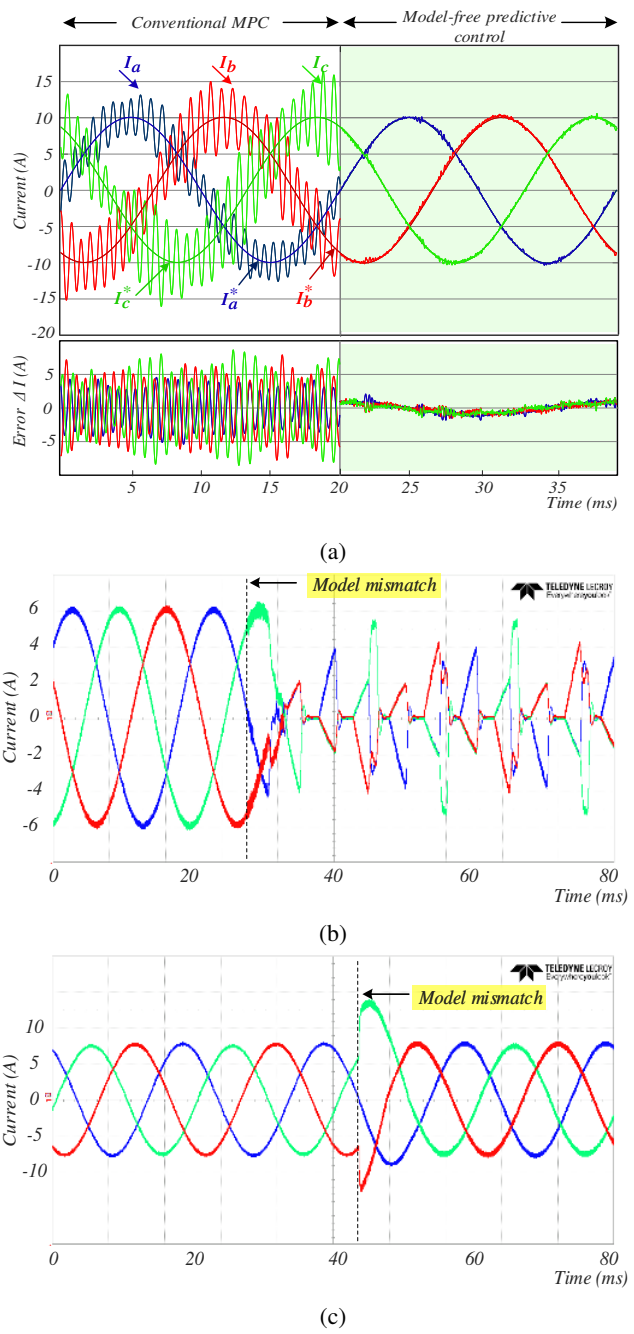

FIGURE 12: Performance comparison of conventional FCS-MPC and the proposed MF-PC of a voltage source inverter considering model mismatch. (a) Simulated comparison between the conventional FCS-MPC and the proposed MF-PC. (b) Experimental validation of the conventional FCS-MPC. (c) Experimental validation of the proposed MF-PC.

also includes the parameter estimation part described in Sec. III-B. Therefore, an increase in the computation time is unavoidable. However, as can be seen in Table 2, the computation time of the proposed MF-PC shows only a slight increase of 6% with respect to the conventional FCS-MPC algorithm. These times were measured in experimental tests with a sampling period of 10 μs, where no overrun events were recorded during the trials.

V. CONCLUSION

This paper has presented a new strategy for predictive current control in a two-level voltage-source inverter without using the physical model and the parameters of the system under

TABLE 2: Computation times of the predictive algorithms.

Algorithm	Computation time (μs)
FCS-MPC	1.831
MF-PC	1.943

control. For this reason, the strategy is named "model-free predictive control". The strategy presented in this paper is based on an estimation of the controlled variables using the Recursive Least Squares (RLS) method which is a standard systems identification technique.

Simulation and experimental results confirm that it is not necessary to have previous knowledge of the physical model of the inverter and the load to apply predictive control. In addition, these results confirm that this new strategy is very robust in relation to parameter and model mismatch in comparison to standard model predictive control.

In the light of these results, it is possible to consider the robust application of predictive control in power electronics systems with higher complexity in a very simple and systematic way, opening a new field of research and industrial application.

REFERENCES

[1] S. Kouro, M. A. Perez, J. Rodriguez, A. M. Llor, and H. A. Young, "Model predictive control: Mpc's role in the evolution of power electronics," *IEEE Industrial Electronics Magazine*, vol. 9, no. 4, pp. 8–21, Dec 2015.

[2] J. M. Guerrero, J. C. Vasquez, J. Matas, L. G. De Vicuña, and M. Castilla, "Hierarchical control of droop-controlled ac and dc microgrids—a general approach toward standardization," *IEEE Trans. Ind. Electron.*, vol. 58, no. 1, pp. 158–172, 2011.

[3] A. Bidram and A. Davoudi, "Hierarchical structure of microgrids control system," *IEEE Trans. Smart Grid*, vol. 3, no. 4, pp. 1963–1976, 2012.

[4] J. Schiffer, T. Seel, J. Raisch, and T. Sezi, "Voltage stability and reactive power sharing in inverter-based microgrids with consensus-based distributed voltage control," *IEEE Trans. Control Syst. Technol.*, vol. 24, no. 1, pp. 96–109, 2016.

[5] Y. Khayat, Q. Shafiee, R. Heydari, M. Naderi, T. Dragičević, J. W. Simpson-Porco, F. Dörfler, M. Fathi, F. Blaabjerg, J. M. Guerrero, and H. Bevrani, "On the secondary control architectures of ac microgrids: An overview," *IEEE Transactions on Power Electronics*, vol. 35, no. 6, pp. 6482–6500, 2020.

[6] R. Heydari, T. Dragicevic, and F. Blaabjerg, "High-bandwidth secondary voltage and frequency control of vsc-based ac microgrid," *IEEE Trans. Power Electrons.*, 2019.

[7] J. Rodriguez, J. Pontt, C. A. Silva, P. Correa, P. Lezana, P. Cortes, and U. Ammann, "Predictive Current Control of a Voltage Source Inverter," *IEEE Trans. on Ind. Electron.*, vol. 54, no. 1, pp. 495–503, Feb 2007.

[8] P. Kou, D. Liang, J. Li, L. Gao, and Q. Ze, "Finite-control-set model predictive control for dfig wind turbines," *IEEE Transactions on Automation Science and Engineering*, vol. 15, no. 3, pp. 1004–1013, 2017.

[9] F. Wang, H. Xie, Q. Chen, S. A. Davari, J. Rodriguez, and R. Kennel, "Parallel Predictive Torque Control for Induction Machines without Weighting Factors," *IEEE Transactions on Power Electronics*, vol. 35, no. 2, pp. 1779–1788, feb 2020.

[10] W. Xu, M. F. Elmorshedy, Y. Liu, J. Rodriguez, and C. Garcia, "Maximum Thrust per Ampere of Linear Induction Machine Based on Finite-Set Model Predictive Direct Thrust Control," *IEEE Transactions on Power Electronics*, vol. 35, no. 7, pp. 7366–7378, jul 2020.

[11] H. Young, M. Perez, and J. Rodriguez, "Analysis of Finite-Control-Set Model Predictive Current Control with Model Parameter Mismatch in a Three-Phase Inverter," *IEEE Transactions on Industrial Electronics*, vol. 63, no. 5, pp. 3100–3107, 2016.

[12] C. Restrepo, G. Garcia, F. Flores-Bahamonde, D. Murillo-Yarce, J. I. Guzman, and M. Rivera, "Current control of the coupled-inductor buck–boost dc–dc switching converter using a model predictive control approach," *IEEE Journal of Emerging and Selected Topics in Power Electronics*, pp. 1–1, 2020.

[13] C. K. Lin, J. T. Yu, L. C. Fu, T. H. Liu, and C. F. Hsiao, "Model-free predictive current controller for four-switch three-phase inverter-fed interior permanent magnet synchronous motor drive systems," in *IEEE/ASME International Conference on Advanced Intelligent Mechatronics, AIM*, 2012, pp. 1048–1053.

[14] C. K. Lin, T. H. Liu, J. T. Yu, L. C. Fu, and C. F. Hsiao, "Model-free predictive current control for interior permanent-magnet synchronous motor drives based on current difference detection technique," *IEEE Transactions on Industrial Electronics*, vol. 61, no. 2, pp. 667–681, 2014.

[15] C. K. Lin, J. T. Yu, Y. S. Lai, and H. C. Yu, "Improved Model-Free Predictive Current Control for Synchronous Reluctance Motor Drives," *IEEE Transactions on Industrial Electronics*, vol. 63, no. 6, pp. 3942–3953, jun 2016.

[16] M. Khalilzadeh, S. Vaez-Zadeh, and M. Eslahi, "Parameter-Free Predictive Control of IPM Motor Drives with Direct Selection of Optimum Inverter Voltage Vectors," *IEEE Journal of Emerging and Selected Topics in Power Electronics*, pp. 1–1, oct 2019.

[17] P. G. Carlet, F. Tinazzi, S. Bolognani, and M. Zigliotto, "An Effective Model-Free Predictive Current Control for Synchronous Reluctance Motor Drives," in *IEEE Transactions on Industry Applications*, vol. 55, no. 4. Institute of Electrical and Electronics Engineers Inc., jul 2019, pp. 3781–3790.

[18] Y. Zhou, H. Li, R. Liu, and J. Mao, "Continuous Voltage Vector Model-Free Predictive Current Control of Surface Mounted Permanent Magnet Synchronous Motor," *IEEE Transactions on Energy Conversion*, vol. 34, no. 2, pp. 899–908, jun 2019.

[19] Y. Zhang, X. Liu, J. Liu, J. Rodriguez, and C. Garcia, "Model-Free Predictive Current Control of Power Converters Based on Ultra-Local Model." Institute of Electrical and Electronics Engineers (IEEE), apr 2020, pp. 1089–1093.

[20] Y. Zhang, J. Jin, and L. Huang, "Model-Free Predictive Current Control of PMSM Drives Based on Extended State Observer Using Ultra-Local Model," *IEEE Transactions on Industrial Electronics*, pp. 1–1, feb 2020.

[21] Z. Chen, J. Qiu, and M. Jin, "Adaptive finite-control-set model predictive current control for IPMSM drives with inductance variation," *IET Electric Power Applications*, vol. 11, no. 5, pp. 874–884, may 2017.

[22] F. Tinazzi, P. G. Carlet, S. Bolognani, and M. Zigliotto, "Motor Parameter-free Predictive Current Control of Synchronous Motors by Recursive Least Square Self-Commissioning Model," *IEEE Transactions on Industrial Electronics*, pp. 1–1, dec 2019.

[23] M. Bermudez, M. R. Arahal, M. J. Duran, and I. Gonzalez-Prieto, "Model Predictive Control of Six-phase Electric Drives Including ARX Disturbance Estimator," *IEEE Transactions on Industrial Electronics*, pp. 1–1, jan 2020.

[24] P. Cortes, J. Rodriguez, D. E. Quevedo, and C. Silva, "Predictive Current Control Strategy With Imposed Load Current Spectrum," *IEEE Transactions on Power Electronics*, vol. 23, no. 2, pp. 612–618, 2008.

[25] J. Slotine and W. LI, *Applied Nonlinear Control*. Prentice Hall, 1991.

[26] H. A. Young, M. A. Perez, and J. Rodriguez, "Analysis of finite-control-set model predictive current control with model parameter mismatch in a three-phase inverter," *IEEE Transactions on Industrial Electronics*, vol. 63, no. 5, pp. 3100–3107, 2016.

[27] R. Heydari, Y. Khayat, A. Amiri, T. Dragicevic, Q. Shafiee, P. Popovski, and F. Blaabjerg, "Robust high-rate secondary control of microgrids with mitigation of communication impairments," *IEEE Transactions on Power Electronics*, pp. 1–1, 2020.

[28] O. Nelles, *Nonlinear System Identification*. Springer-Verlag, 2001.

[29] S. Yuan, H. Wu, and C. Yin, "State of Charge Estimation Using the Extended Kalman Filter for Battery Management Systems Based on the ARX Battery Model," *Energies*, vol. 6, no. 1, pp. 444–470, jan 2013. [Online]. Available: http://www.mdpi.com/1996-1073/6/1/444

[30] S. L. Shah and W. R. Cluett, "Recursive least squares based estimation schemes for self-tuning control," *The Canadian Journal of Chemical Engineering*, vol. 69, no. 1, pp. 89–96, feb 1991. [Online]. Available: http://doi.wiley.com/10.1002/cjce.5450690111

[31] D. J. Park, B. E. Jun, and J. H. Kim, "Fast tracking rls algorithm using novel variable forgetting factor with unity zone," *Electronics Letters*, vol. 27, no. 23, pp. 2150–2151, oct 1991.

[32] Q. Shafiee, J. M. Guerrero, and J. C. Vasquez, "Distributed secondary control for islanded microgrids—a novel approach," *IEEE Trans. Power Electron.*, vol. 29, no. 2, pp. 1018–1031, 2014.

This article has been accepted for publication in a future issue of this journal, but has not been fully edited. Content may change prior to final publication. Citation information: DOI 10.1109/ACCESS.2020.3039050, IEEE Access

JOSÉ RODRÍGUEZ (M'81-SM'94-F'10) received the Engineer degree in electrical engineering from the Universidad Tecnica Federico Santa Maria, in Valparaiso, Chile, in 1977 and the Dr.-Ing. degree in electrical engineering from the University of Erlangen, Erlangen, Germany, in 1985. He has been with the Department of Electronics Engineering, Universidad Tecnica Federico Santa Maria, since 1977, where he was full Professor and President. Since 2015 he was the President and since 2019 he is full professor at Universidad Andres Bello in Santiago, Chile. He has coauthored two books, several book chapters and more than 400 journal and conference papers. His main research interests include multilevel inverters, new converter topologies, control of power converters, and adjustable-speed drives. He has received a number of best paper awards from journals of the IEEE. Dr. Rodriguez is member of the Chilean Academy of Engineering. In 2014 he received the National Award of Applied Sciences and Technology from the government of Chile. In 2015 he received the Eugene Mittelmann Award from the Industrial Electronics Society of the IEEE. In years 2014 to 2019 he has been included in the list of Highly Cited Researchers published by Web of Science.

RASOOL HEYDARI (S'16-M'19) received the Ph.D. degree in electrical engineering from the Department of Energy Technology, Aalborg University, Denmark, in 2019, where he focused on several research activities related to power electronic-based power systems, under the supervision of Prof. F. Blaabjerg. He was also a visiting researcher with ABB Corporate Research Center, Västerås, Sweden, in 2019. He is currently a Post-Doctoral Fellow with the Department of Electrical Engineering, the Mads Clausen Institute, University of Southern Denmark, Odense, Denmark. His principal field of interest include control, stability and dynamic analysis of power electronic systems, mainly distributed and grid-connected converters, microgrid, and low-inertia power grids. Dr. Heydari serves as a Reviewer with several journals, including IEEE Transactions on Power Electronics, the IEEE Transactions on Industrial Electronics, and the IET Power Electronics.

ZAHRA RAFIEE received her B.Sc. and M.Sc. degree in Power Electrical Engineering from the Department of Electrical Engineering, Bu Ali Sina University, Hamadan Iran, in 2006 and 2010, respectively. She studies Ph.D. in Electrical Engineering at Shahid Beheshti University. Her research interests are stability in power system, protection of network, optimization control algorithms, application of neural network, and fuzzy logic in the power system.

HECTOR A. YOUNG (S'12–M'15) was born in Valparaiso, Chile in 1984. He received the B.Eng. and the M.Sc. degrees in electronics engineering in 2009 from the Universidad de la Frontera, Temuco, Chile. He received the PhD degree in power electronics from the Universidad Tecnica Federico Santa Maria, Valparaiso, Chile in 2014.

From 2014 he has been an Assistant Professor with the Electrical Engineering Department, Universidad de La Frontera. His research interests include modeling and control of power converters and electrical drives, renewable energy systems and microgrids.

FREDDY FLORES-BAHAMONDE was born in Osorno, Chile in 1983. He received the M.Sc. and Ph.D degrees in electronics engineering from Universitat Rovira i Virgili (URV), Tarragona, Spain, in 2009 and 2013, respectively. In 2015 he joined to the Advanced center for electrical and electronic engineering (AC3E), from the Universidad Técnica Federico Santa María (UTFSM), Valparaíso, Chile, as a postdoctoral fellow. In 2017 he was in charge of the energy area in the technology transfer unit of the AC3E developing and managing industrial projects related to the energy and electric power systems field.

Dr. Flores-Bahamonde is currently Assistant Professor in the Engineering Sciences Department at the Universidad Andrés Bello, where he is also researcher in the Energy Transformation Center. His main interest includes the design and control of power converters for renewable energies, automotive power systems, and DC microgrids.

MAHDI SHAHPARASTI (S'08, SM'20) received the Ph.D. degree in electrical engineering specializing in power electronics from Tarbiat Modares University, Tehran, Iran, in 2014. For 7 years, between 2010-2014 and 2016-2017, he was a Research and Development Researcher with JDEVS Company, Tehran, designing medium and high power converters. Moreover, in 2016, he served as an assistant professor with the Department of Electrical Engineering, East Tehran Branch, Islamic Azad University, Tehran. During 2015 and 2017-2019, he was a Postdoctoral Researcher with the Technical University of Catalonia, Barcelona, Spain, where he is involved in the control of high power grid-connected converters. He is currently a postdoc at the University of Southern Denmark. His current research interests include control standalone and grid-connected inverters, renewable energy resources, and motor drive systems.